Longitudinal Follow-up of Cardiac Structure and Functional Changes in an Infarct Mouse Model Using Retrospectively Gated Micro-Computed Tomography

Sarah A. Detombe, BSc,† Nancy L. Ford, PhD,‡ Fuli Xiang, MD,§ Xiangru Lu,¶ Qingping Feng, MD, PhD,§¶‖ and Maria Drangova, PhD*†*

Objectives: Mouse models of myocardial infarction are valuable in studying the effect of genetic modifications on structural and functional remodeling of the heart. Our group recently developed a method for acquiring three-dimensional images of the beating mouse heart using micro-computed tomography (micro-CT) and retrospective gating. In this study, we evaluated cardiac function in sham and infarcted mice longitudinally, using this novel technique.

Materials and Methods: Thirteen mice (7 sham-operated, 6 infarcted; male, C57BL/6) were imaged at baseline and at weeks 1, 2, 3, and 4 postligation of the left anterior descending coronary artery. Animals were anesthetized with 1.5% isoflurane; mechanical ventilation was not used. Contrast between blood and tissue was provided by an iodinated blood-pool contrast agent (0.01 mL/g Fenestra VC). The cardiac and respiratory waveforms were recorded during the 50-second scan time, to enable retrospective gating. Once scanning was completed on week 4 postsurgery, hemodynamic measurements were performed using a Millar pressure conductance catheter.

Results: There were significant differences in systolic and diastolic volumes, and ejection fraction, between sham and myocardial infarction groups ($P < 0.0001$). A comparison of ejection fraction derived from both CT and hemodynamic measurements was not significantly different ($P > 0.1$).

Conclusions: We have demonstrated the first use of dynamic micro-CT for monitoring cardiac remodeling, resulting from myocardial infarction, over time. The fast scan times (<1 minute) and ability to track individual animals over an entire study make this quantitative noninvasive technique a promising tool for in vivo studies of cardiac disease in mouse models.

Key Words: heart failure, imaging, myocardial infarction, remodeling, micro-computed tomography

(*Invest Radiol* 2008;43: 520–529)

Mouse models have become increasingly important in the study of cardiovascular diseases. Detailed information about the genome has allowed models to be developed that either overexpress or underexpress specific genes to study their contribution to the pathophysiology of a given cardiovascular disease process.

The established method for studying cardiac function in mouse models involves the analysis of pressure-volume relationships measured using a pressure-conductance catheter. By inserting a catheter into the left ventricle (LV) and recording both pressure and volume readouts, heart function can be determined, most notably by detecting small alterations in myocardial contractility.[1] However, because of the inability of pressure-volume conductance devices to continuously measure parallel conductance, LV volume is often underestimated.[2,3] The procedure is also invasive, resulting in a terminal experiment, and requires an individual with specialized surgical skill to produce consistent data.

Multiple imaging modalities have been developed that have the capability of measuring cardiac structure and function in the mouse; these are noninvasive procedures that allow individual animals to be tracked over the entire study. Commonly used techniques are magnetic resonance imaging (MRI)[4–10] and echocardiography,[11–16] both of which have been used to successfully measure LV function. MR images typically require long scan times and are usually acquired with large slice thicknesses (~1 mm). Accurate heart function measurements also require that the scans be acquired in the short axis orientation, which can be difficult to define in diseased hearts,[5] although a recent study[17] has described a

Received November 15, 2007 and accepted for publication, after revision, March 3, 2008.

From the *Imaging Research Laboratories, Robarts Research Institute, University of Western Ontario, London, Ontario, Canada; †Department of Medical Biophysics, University of Western Ontario, London, Ontario, Canada; ‡Department of Physics, Ryerson University, Toronto, Ontario, Canada; §Department of Medicine, University of Western Ontario, London, Ontario, Canada; ¶Lawson Health Research Institute, London, Ontario, Canada; and ‖Department of Pharmacology and Toxicology, University of Western Ontario, London, Ontario, Canada.

Supported by the Heart and Stroke Foundation of Ontario (NA 5578). Partial support was also provided by the Ontario Research and Development Challenge Fund. Sarah Detombe is funded by a Heart and Stroke Foundation of Ontario (HSFO) Master's Studentship and a Canadian Institute of Health Research Strategic Training Program in Vascular Research. Maria Drangova and Qingping Feng are HSFO Career Investigators.

Reprints: Maria Drangova, PhD, Imaging Research Laboratories, Robarts Research Institute, P.O. Box 5015, 100 Perth Dr., London, ON N6A 5K8, Canada. E-mail: Maria.Drangova@imaging.robarts.ca.

ISSN: 0020-9996/08/4307-0520

method of acquiring three-dimensional (3D) MR images with 200-μm isotropic voxels, which may alleviate this limitation.

Echocardiography is frequently used because it is easy to operate, can provide real-time images, and can measure velocity. Although two-dimensional (2D) imaging is available (and 3D imaging has been demonstrated[18]), cardiac function is most frequently measured from M-mode images.[12,19–21] Estimating cardiac function from M-mode and 2D images relies on geometrical assumptions and is highly user dependent.

In recent years, micro-computed tomography (micro-CT) techniques have emerged, capable of overcoming the challenges of imaging the mouse heart such as the fast heart rate (about 500 beats per minute under anesthetic) and the small size (5 mm across the short axis of the ventricle). Badea et al[22] demonstrated a prospectively gated micro-CT technique that acquires 3D images with 90-μm isotropic voxels, and a scan time of approximately 10 minutes for each cardiac phase, which has recently been applied to an infarct mouse model.[23] This technique, however, requires that the animals be intubated, and mice are scanned in a vertical position, which may disrupt cardiac function.[24]

Retrospectively gated micro-CT imaging techniques have been recently developed that enable the acquisition of 3D images throughout the cardiac cycle in free-breathing mice.[25,26] The methodology outlined by Drangova et al[25] has multiple advantages, including a short scan time ($<$1 minute), and high resolution (150-μm isotropic voxel spacing). Retrospectively gated micro-CT can provide both quantitative and qualitative assessment of cardiac function that, as a result of the minimal anesthetic required and the short scan times, offers nominal disruption to the animal. In this study, we follow heart failure progression in an infarct mouse model over 4 weeks to demonstrate the utility of this technique when investigating a mouse model of cardiovascular disease. To the best of our knowledge, this is the first study using retrospectively gated micro-CT to follow cardiac remodeling in each individual mouse over time following the induction of an infarct.

MATERIALS AND METHODS

All studies performed were approved by the Animal Use Subcommittee of the University Council on Animal Care at our institution. Fourteen male C57BL/6 mice, approximately 25-weeks-old and weighing 32 $\pm$ 3 g, were split into 2 groups; one group underwent ligation of the left coronary artery, and the other group underwent sham surgery. Mice were scanned at baseline (before surgery), and at weeks 1, 2, 3, and 4 postsurgery; 3 of the sham mice and 3 of the myocardial infarction (MI) mice did not receive a scan at baseline and week 2 postsurgery.

Induction of Myocardial Infarction

Surgery was performed as previously described.[27] Animals were anesthetized with ketamine (50 mg/kg) and xylazine (12.5 mg/kg) delivered intraperitoneally. The mice were then intubated and artificially ventilated. A left thoracotomy was performed, exposing the LV wall; the left coronary artery was ligated by positioning a suture between the pulmonary artery out-flow tract and the left atrium. Sham-operated animals underwent the same surgical procedure, including positioning of the suture, but it was not tightened to ligate the artery. To decrease acute mortality after ligation, atropine (0.05 mg subcutaneous) was administered before surgery to decrease airway excretion. After surgery, mice were treated with antibiotic agent (oxytetracycline, 200 mg/L) via drinking water for 3 days; analgesic (0.03 mg/kg buprenorphine subcutaneous) was administered to relieve pain.

Animal Preparation for Scanning

Mice were anesthetized with 1.5% isoflurane in O_2. Approximately 5 minutes before scanning, the animals were injected intravenously with 0.01 mL/g Fenestra VC (50 mg I/mL; Advanced Research Technologies, Inc., St. Laurent, Quebec, Canada), an iodinated blood-pool contrast agent that enhances the vasculature for several hours.[28] The dose given in this study was half the dose administered by Drangova et al[25] and Badea et al[22] This dose of contrast agent was selected to reduce the volume injected into the mice, and pilot experiments demonstrated that sufficient contrast was achieved at this dose level.[28] Three neonatal electrocardiogram electrodes (2269T; 3M Health Care, St. Paul, MN) were attached to the paws, and the animals were separately placed prone on a respiratory monitoring bed connected to a pressure transducer, which translates diaphragm motion to a recording of a respiratory wave signal.[29] Physiological signals were recorded using a physiological monitoring and triggering system (BioVet; m2m Imaging Corp., Newark, NJ). Temperature was monitored and maintained between 36°C and 37°C for all scans. The mice were not intubated and remained free breathing during the experiment.

Image Acquisition and Retrospective Gating

Images were acquired using a volumetric cone-beam micro-CT scanner (Locus Ultra; General Electric Healthcare, London, Ontario, Canada), equipped with a flat-panel detector and clinical x-ray tube mounted on a slip-ring gantry, which enables continuous dynamic acquisition of x-ray projections. Projection images were acquired at 80 kVp and 50 mA over a field of view measuring 14 cm (transaxial) $\times$ 5.4 cm (longitudinal). To enable retrospective gating, projections were acquired over 10 rotations (5 seconds per rotation, 416 projection images per rotation at a rate of 12 ms/projection) for a total scan time of 50 seconds. Entrance dose for a 50-second scan was previously calculated to be 0.28 Gy.[25]

Retrospective gating and reconstruction of acquired projection images is described in detail by Drangova et al[25] Briefly, for each phase of the cardiac cycle projections were selected, from those acquired, based on the recorded respiratory and electrocardiogram signals; only projections occurring during end expiration and a predetermined cardiac window (12 milliseconds) were used to reconstruct the 3D image for the selected cardiac phase. For this study, 9–13 3D images were reconstructed per cardiac cycle, depending on the heart rate. All images were reconstructed on a 256 $\times$ 256 $\times$ 360 matrix with isotropic voxel spacing of 150 μm $\times$ 150 μm $\times$ 150 μm.[30]

Image Analysis

Image analysis was performed using MicroView software (version ABA 2.2; General Electric Healthcare). Images were reoriented to align with the long and short axes of the heart. To calculate LV volume, an automated seeded region-growing algorithm was used. First, a threshold level that separated the blood from the myocardium in the images was identified automatically[31] by drawing small regions of interest containing equal parts of tissue and blood. Because of small differences in the concentration of contrast agent in each mouse at scan time, a separate threshold value was defined for each animal at each time point. Automatic region growing was then used to segment the LV chamber from the myocardium; the region growing was terminated at the aortic valve, with manually drawn contours limiting the segmentation near the valve where the wall of the ventricle became too thin to constrain the region-growing algorithm. The aortic valve was visually located in the short axis plane and the anatomic location was confirmed in the coronal view. LV volume was calculated based on the segmented region and the known voxel size. Systolic and diastolic images were identified by calculating LV volume throughout the cardiac cycle to determine the frames that had minimum and maximum volumes. Once the left-ventricular systolic volume (LVSV) and the left-ventricular diastolic volume (LVDV) were determined, stroke volume (SV = LVDV − LVSV), ejection fraction (EF = SV/LVDV), and cardiac output (CO = SV × heart rate) were calculated.

LV Mass Measurements

LV mass was determined from the CT images for all mice in weeks 1 and 4. A contour was manually drawn around the outer edge of the LV, using the aortic valve as an upper boundary, and the LV wall was automatically segmented within the contoured region using the threshold previously calculated for LV chamber volume determination. The resulting myocardium volumes were multiplied by the density of myocardium (1.05 g/mL) to calculate LV mass.

Reproducibility

The reproducibility of the technique was determined in terms of interobserver, intraobserver, and intrasubject variability. For interobserver variability, the systolic and diastolic images of 13 mice (7 sham and 6 MI), acquired at weeks 1 and 4 postsurgery, were analyzed by three independent operators. Intraobserver variability was determined by one individual analyzing these same images three times. For intrasubject variability determination, 2 sham and 3 MI mice were each scanned three times, after repositioning, at the final scan time-point (4 weeks).

Hemodynamic Measurements

Hemodynamic measurements were performed as previously described[27]: after scanning at the 4-week time-point, mice were anesthetized with sodium pentobarbital (50 mg/kg IP), and a Millar pressure conductance catheter (model SPR-839, 1.4 F) was inserted into the LV via the right carotid artery to measure LV pressures, volumes, and heart rate. Data were recorded by a PowerLab Chart program (ADInstruments, Inc., Colorado Springs, CO). All hemodynamic parameters were analyzed by a PVAN software (Millar Instruments, Houston, TX). After hemodynamic analysis, hearts were excised, fixed with 10% formalin, then sliced and stained with hematoxylin and eosin.

Statistical Analysis

Data are presented as mean ± standard deviation. Two-way analysis of variance was performed, using Prism 4 (GraphPad Software, Inc., San Diego, CA), to compare differences between sham and MI groups over time for each of the cardiac functional parameters (LVSV, LVDV, SV, EF, CO). Variabilities were calculated as the standard deviations of the means of multiple measurements. Power tests were performed using StatMate 2 (GraphPad Software, Inc.). Results were considered statistically significant at $P < 0.05$.

RESULTS

Retrospectively gated micro-CT images were successfully acquired in all 14 mice; one mouse was excluded from analysis retrospectively because of unsuccessful ligation of the coronary artery, which failed to create an infarct. On average, the contrast agent increased the attenuation of the blood pool to 331 ± 57 Hounsfield unit (HU), compared with the myocardial tissue (76 ± 27 HU); the average threshold that separated the blood pool in the LV from the myocardium was 255 ± 54 HU. Out of 416 possible projections, an average of 325 ± 42 projections were available to reconstruct an image at each point in the cardiac cycle. The average noise in the myocardium was previously measured to be 36 ± 4.6 HU.[25]

Figure 1 shows representative long- and short-axis images acquired at week 4 postsurgery in a sham-operated (Figs. 1A, C) and an MI (Figs. 1B, D) mouse. The images were extracted from the 3D images reconstructed at the selected phase of the cardiac cycle. The infarcted heart (Fig. 1B) is distended, with a thinning of the wall in the apex of the ventricle, representing the infarct (noted with arrows). Note the entire heart of the MI mouse appears to be enlarged. Figure 2 shows the histology of the LV from an MI (A) and a sham (B) mouse at week 4 postsurgery. The enlarged LV from the MI mouse and the area of infarction are clearly demonstrated.

Figures 3A (sham-operated) and B (infarct model) represent long- and short-axis views of an individual mouse heart in diastole (i, iii) and systole (ii, iv). Apparent from these images are the differences in size between systole and diastole when comparing sham and MI animals. Figures 4 and 5 illustrate differences in cardiac morphology of a heart in diastole in a sham-operated and an MI mouse, respectively, over the course of the experiment. The size and shape difference between baseline and the final time point is also demonstrated in the 3D representation of the LV chambers of an MI mouse shown in Figure 6.

One of the main advantages of using a noninvasive imaging technique includes the ability to quantify changes in cardiac function in individual animals over time. Figure 7(A–E) illustrates the functional parameters calculated for individual mice and Figure 7F tracks the measured heart

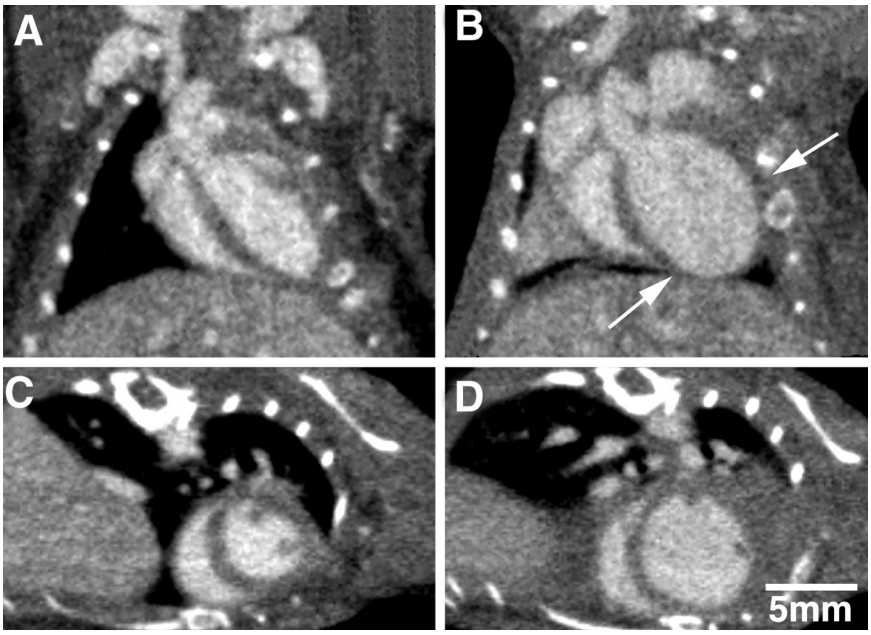

FIGURE 1. Long (A, B) and short (C, D) axis images of the mouse heart in diastole of a sham-operated (A, C) and an MI (B, D) mouse. These images represent 150-μm sections taken from the reconstructed 3D volumes. The in-plane voxel spacing is also 150 μm. Note that the entire heart of the MI mouse is enlarged, indicating the global effects of the infarct. The infarct is evident in the thinned wall in the apex of the LV, below the arrows.

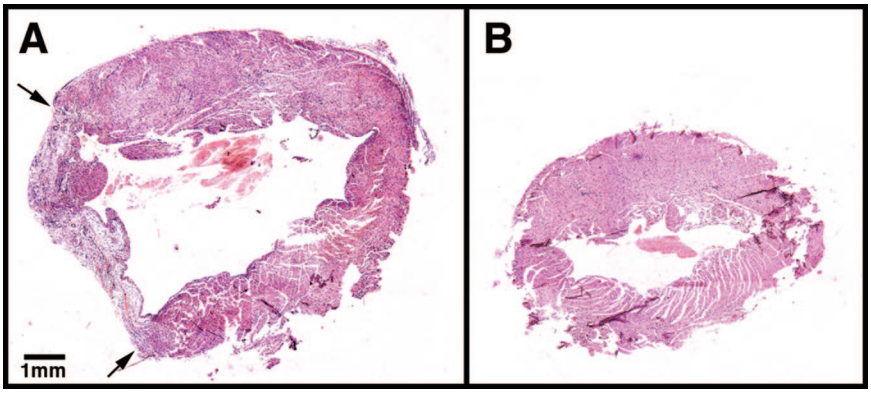

FIGURE 2. Histologic slides of the LV from an MI (A) and a sham (B) mouse, stained with hematoxylin and eosin. The infarct is identified by arrows in (A).

rates. Note the small weekly changes observed in individual mice in LVSV (Fig. 7A) and LVDV (Fig. 7B), as well as in the functional parameters calculated from the volumes. Average values of the functional parameters for each week were also calculated and are listed in Table 1. Significant differences ($P < 0.0001$) were observed between the sham and MI groups for LVSV, LVDV, and EF, as demonstrated by 2-way analysis of variance; also, LVSV and LVDV showed significant differences over time ($P < 0.0001$). SV and CO did not show significant differences either between the surgery groups or over time ($P > 0.1$ for all tests). Power tests determined there was sufficient power (>80%) to detect expected differences[18,23,32] in LVSV, LVDV, and EF. Power calculations for SV and CO showed insufficient power to detect differences of 20%, which have been previously observed between sham and MI mice.[33]

LV mass measurements calculated from the CT images are listed in Table 2. Significant differences were seen between the sham and MI groups in both weeks 1 and 4 ($P = 0.012$ and 0.008, respectively); changes in LV mass between weeks 1 and 4 were insignificant for both the sham ($P = 0.60$) and MI ($P = 0.08$) groups.

Variability studies showed excellent reproducibility of measurements between individuals, and by the same individual (Table 3). Intrasubject measurements also show good reproducibility, with variation in volumes of infarcted hearts being slightly higher than variations in sham-operated hearts (Table 3). Overall, the variability due to image analysis by the same or different observers was low (on average, less than ± 0.85 and ± 1.8 μL, respectively) and was lower than the intrasubject variability in LV volumes (± 2.8 μL on average).

Hemodynamic measurements made in week 4 (Table 4) were compared with measurements made from CT images. Comparison of the ejection fractions measured using the two techniques showed no significant differences for either the sham or the MI groups ($P > 0.1$).

DISCUSSION

This study is the first to demonstrate longitudinal tracking of quantitative cardiac functional parameters in individual

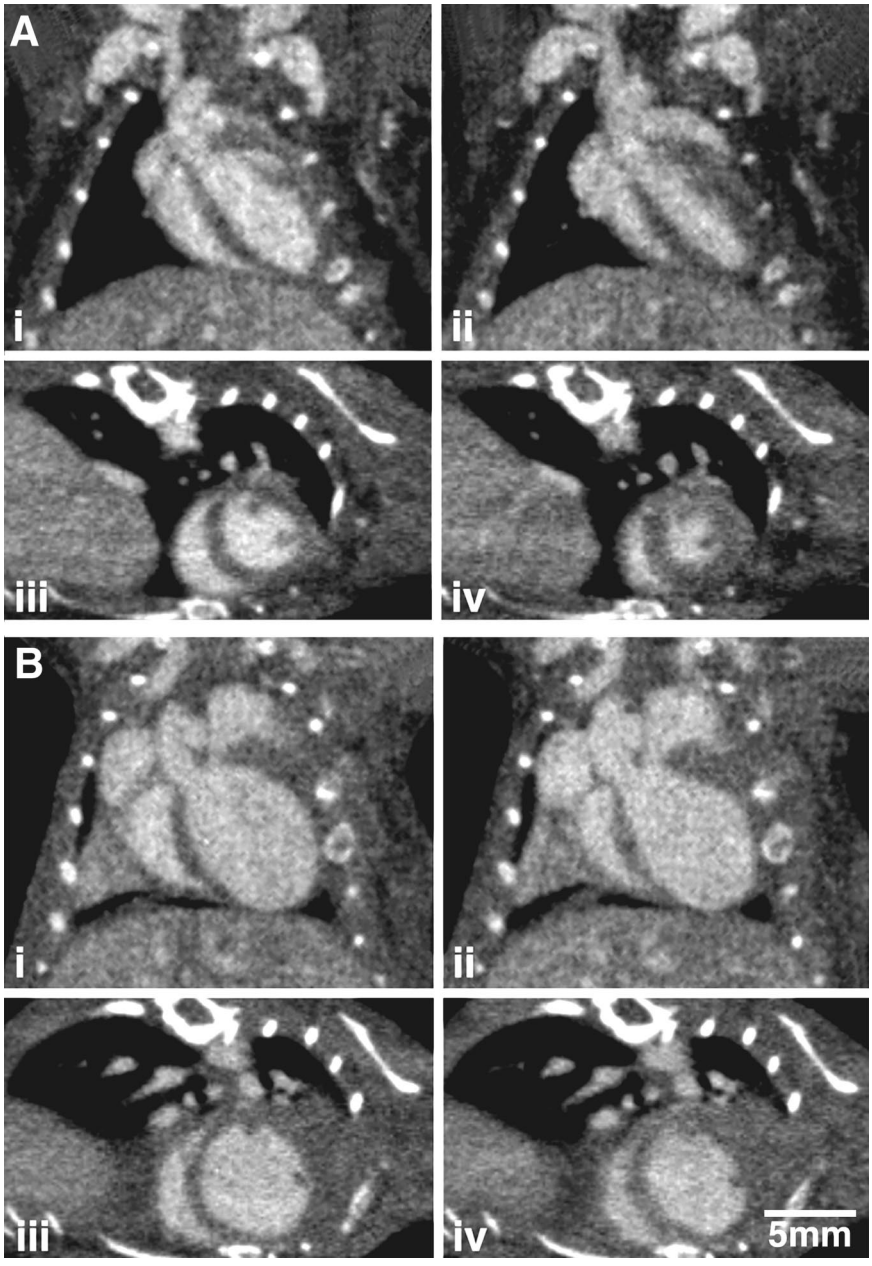

FIGURE 3. Long- and short-axis images of a sham-operated mouse heart (A) and a MI mouse heart (B) in diastole (i, iii) and systole (ii, iv). The images were acquired 4 weeks postsurgery. Note the obvious reduction in contraction of the infarcted heart (B) compared with the sham-operated heart (A).

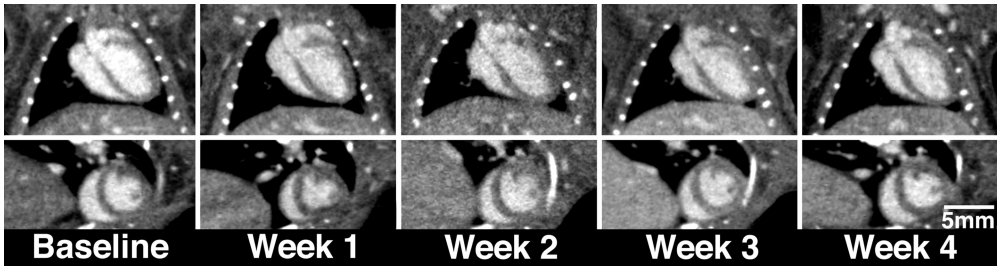

FIGURE 4. A series of long and short axis images showing weekly changes in a sham-operated mouse heart in diastole. Time points represented are baseline, 1 week postsurgery, 2 weeks postsurgery, 3 weeks postsurgery, and 4 weeks postsurgery.

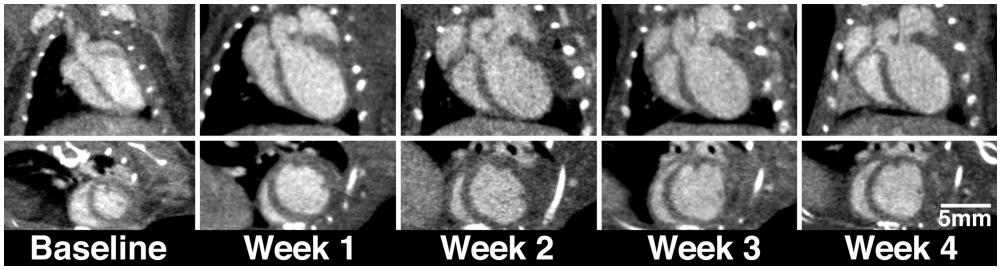

FIGURE 5. A series of long and short axis images showing weekly changes in a MI mouse heart in diastole. Time points represented are baseline, 1 week postsurgery, 2 weeks postsurgery, 3 weeks postsurgery, and 4 weeks postsurgery.

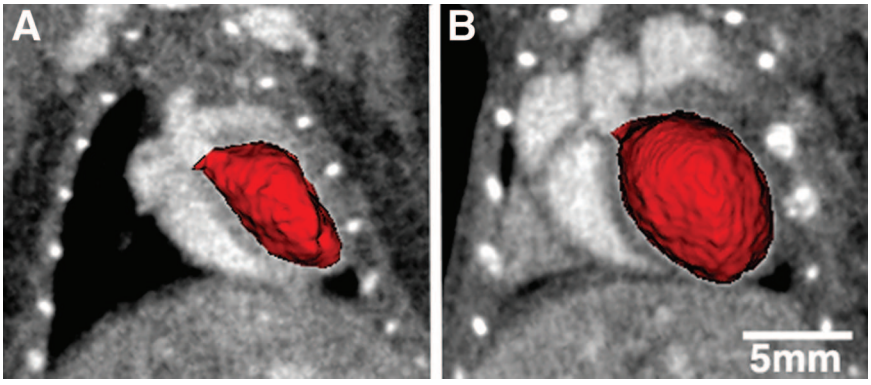

FIGURE 6. 3D representation (isosurface) of the LV overlaid on images of an infarcted heart at baseline (A) and week-4 postinfarction (B). The isosurface models were generated from wire-frame meshes created after an intensity-based region growing operation.

mice using a dynamic micro-CT scanner. Recently published data demonstrated in healthy mice that retrospectively gated micro-CT rapidly and reproducibly acquires images that can be used to quantify cardiac function.[25] Retrospectively gated micro-CT takes advantage of the scanning capabilities of a volumetric CT scanner equipped with a 2D detector mounted on a slip-ring gantry, making continuous image acquisition possible. Contrast between blood and myocardium is provided by a tri-iodinated blood-pool contrast agent, which provides excellent contrast for several hours.[28] The entrance dose of 0.28 Gy per scan, although higher than the dose reported for clinical diagnostic CT thorax exams,[34,35] is not anticipated to have a detrimental effect on cardiovascular physiology in the mouse.[25,36,37] The advantages of this micro-CT scanning method include: (1) scan times of less than 1 minute to characterize cardiac function over the entire cycle, by generating a series of high-resolution (150 μm isotropic voxels) 3D images; (2) the capability of scanning free-breathing animals in a prone position and; (3) the ability to scan animals under very light anesthesia (typically provided by isoflurane, which has little effect on cardiac function when compared with injectable anesthetics[38–41]).

This current study endeavored to demonstrate that retrospectively gated micro-CT precisely identifies the differences in heart function between infarcted and control mice and can follow these differences longitudinally in individual mice. Differences in cardiac structure were clearly identifiable in the 3D images (Fig. 1), where infarcted mice demonstrated drastically enlarged hearts and thinned walls in the apical 40% of the LV (arrows Fig. 1B); the enlarged right ventricle and atria illustrate the widespread effect of the infarct. Histologic slides of the LV from an MI mouse and a sham mouse (Fig. 2) confirm the enlarged size and the area of infarction identified on the CT images. Quantitative differences in LV size and function were also observed between the sham and MI groups at all time points in the study (Table 1). Significant differences were observed for systolic and diastolic LV volumes, and for ejection fraction between the two groups at all time points postsurgery. Significant increases in LV size with time over the course of the experiment were also observed in the MI mice (Fig. 7A, B).

Baseline EF values were lower than expected for healthy mice.[17,23,32] It was necessary to transport the mice between facilities for the baseline scans, whereas for weeks 1–4, the animals were housed in the same building as the scanner; at the time, this was an unavoidable complication of the study. The transportation may have caused a low level of stress in the mice, resulting in abnormally low ejection fractions.[42,43] The unexpected results highlight an advantage of this micro-CT technique: the ability to closely track perturbations in the animal's health during a study that would have otherwise been undetected. These results also suggest that transportation of mice before imaging, or other study that measures physiological function, should be avoided on the day of the procedure.

On average, the measured values for CO agreed with previously reported results at the experimental end point.[32,33] The lack of significant differences in SV and CO between the sham and MI groups is potentially attributable to the limited time frame over which the experiment was carried out; although the EF was clearly reduced in the MI mice, the compensatory increase in heart size may be responsible for

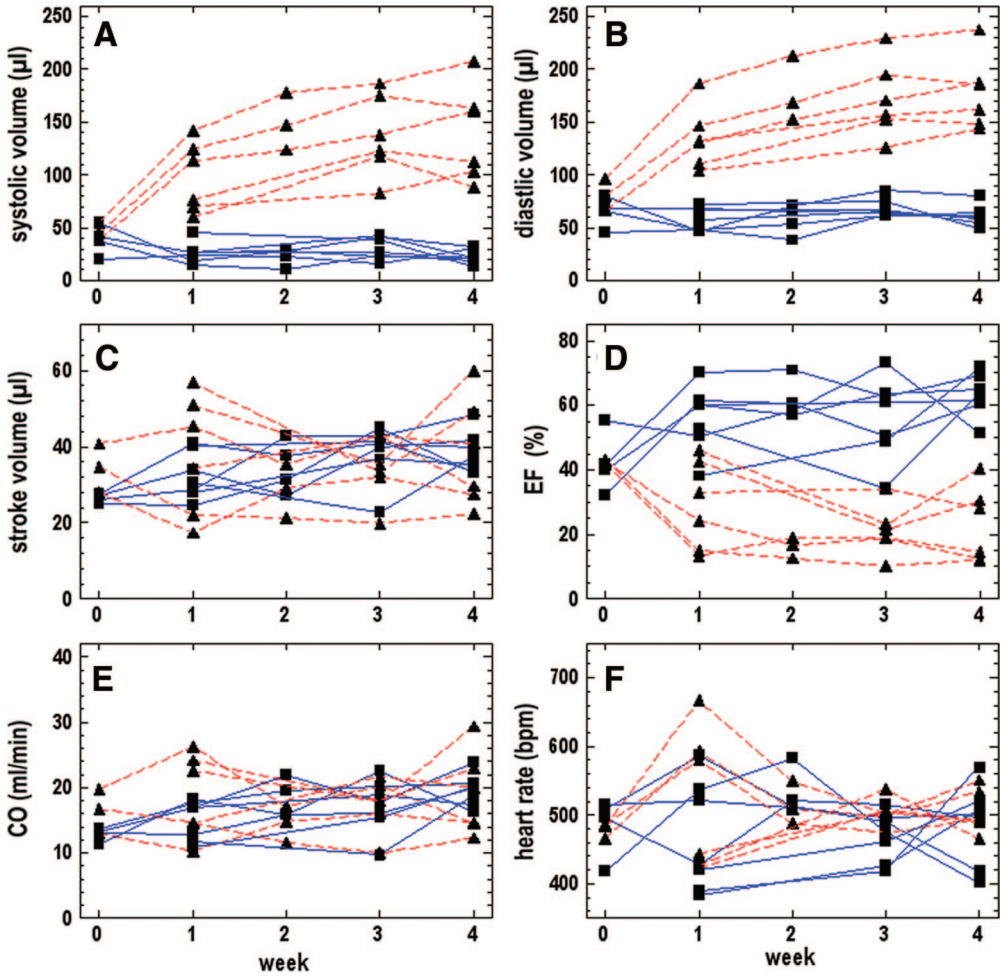

FIGURE 7. Measured cardiac functional parameters tracking individual mice over the 5-week experiment. Graphs represent systolic volume (A), diastolic volume (B), stroke volume (C), ejection fraction (D), cardiac output (E), and heart rate (F). Sham-operated mice are represented by blue solid lines and squares; MI mice are represented by red dashed lines and triangles. Note that each symbol represents the measurements of an individual mouse at each time point.

the maintenance of a relatively constant stroke volume, and therefore, cardiac output. Similar increases in cardiac dimension were reported by Yang et al[44] who used echocardiography to measure LV diastolic shortening in different groups of infarcted mice, which were killed at each experimental time point.

An important advantage of tracking the same animal over the entire course of an experiment using a noninvasive imaging technique is that small changes in individual animals are not lost in the averaging process of a population of mice; a baseline scan can act as the ideal control for the animal at later time points, and paired statistical analyses can be performed. This advantage is seen qualitatively in the series of images in Figure 5, which depict the gradual cardiac remodeling as it occurs over the 4 weeks, and quantitatively in Figure 7.

LV mass measurements are an important element of tracking changes to the myocardium. In this study, we determined LV mass in both groups of mice at weeks 1 and 4 (Table 2). A significant difference in mass between the sham and MI groups was observed, confirming that hypertrophy had occurred after the induction of the infarct; there was no significant difference between the weeks, indicating that the observed hypertrophy took place during the first week after surgery.

The variability studies demonstrated that overall the quantitative measurements were highly reproducible. Because most of the analysis was automatic, both inter- and intraobserver variability depended mostly on the variability of contour placement in the regions near the base of the LV. The excellent intrasubject variability (repeated scans on the same mouse in the same scanning session) provided further support that the low EF measurements made at baseline reflect true physiologic changes. The intrasubject variability was slightly higher for the MI mice than the sham-operated mice; this difference was attributed to the rounded shape of the LV in infarcted mice making the identification of the base of the heart more subjective. The ability to reorient the high-resolution 3D isotropic images to align with the long- and short-axis of the hearts improves the ease of identifying

TABLE 1. Weekly Average Functional Parameters of Sham-Operated and MI Groups

	Functional Parameter				
	LVSV (μL)	**LVDV (μL)**	**SV (μL)**	**EF (%)**	**CO (mL/min)**
Baseline					
Sham (4)	38.5 ± 14.1	65.1 ± 14.7	26.5 ± 1.1	42.4 ± 9.5	12.9 ± 1.0
MI (3)	46.5 ± 8.2	81.0 ± 14.7	34.5 ± 6.5	42.5 ± 1.0	16.5 ± 3.4
P	ns	ns	ns	ns	ns
Week 1					
Sham (7)	26.1 ± 9.7	58.6 ± 10.9	32.4 ± 6.3	56.2 ± 10.2	15.0 ± 3.1
MI (6)	97.5 ± 33.3	135.2 ± 29.6	37.8 ± 15.9	29.0 ± 13.8	18.8 ± 6.4
P	0.0002	<0.0001	ns	0.0018	ns
Week 2					
Sham (4)	22.3 ± 7.9	57.1 ± 14.5	34.7 ± 7.0	61.8 ± 6.2	18.3 ± 3.0
MI (3)	149.4 ± 27.1	177.9 ± 31.2	28.5 ± 7.1	16.1 ± 3.3	14.5 ± 2.8
P	0.0003	0.0009	ns	<0.0001	ns
Week 3					
Sham (7)	30.5 ± 10.5	68.9 ± 8.3	38.4 ± 7.4	56.3 ± 12.7	17.3 ± 4.1
MI (6)	137.0 ± 38.4	171.5 ± 36.2	34.4 ± 8.5	21.1 ± 7.8	17.3 ± 4.1
P	<0.0001	<0.0001	ns	0.0001	ns
Week 4					
Sham (7)	22.7 ± 6.5	61.3 ± 9.7	38.5 ± 5.5	63.3 ± 6.6	19.6 ± 2.4
MI (6)	139.3 ± 45.4	177.5 ± 34.6	38.2 ± 14.5	23.1 ± 11.7	19.0 ± 6.5
P	<0.0001	<0.0001	ns	<0.0001	ns

Values are means ± SD.
ns indicates not significant; numbers in brackets represent number of animals.

TABLE 2. Average LV Mass Measurements for Sham and MI Groups in Weeks 1 and 4 Postsurgery

	LV Mass (mg)		
Group	**Week 1**	**Week 4**	***P***
Sham mice (n = 7)	91 ± 14	101 ± 14	ns
MI mice (n = 6)	122 ± 23	136 ± 24	ns
P	0.012	0.008	

Values are means ± SD. n indicates number of animals.

the base of the heart, where manually drawn contours were required. This is in contrast to most MRI and echocardiography experiments, where the images must be acquired in the short axis of the heart, which can be difficult, especially in remodeled hearts.[5] Note that retrospective reorientation of MR or echocardiographic images acquired with thicker slices (~1 mm) or large interslice spacing (in the case of 3D echo) is typically not possible; the voxels are not isotropic and reorienting would introduce interpolation effects.

Limitations

One of the limitations of this study was the inability to directly compare CT-derived measurements with the catheter-

TABLE 3. Average Interobserver, Intraobserver, and Intrasubject Variabilities of Systolic and Diastolic Volumes

	Sham Mice		MI Mice	
	Systole (μL)	**Diastole (μL)**	**Systole (μL)**	**Diastole (μL)**
Interobserver	(n = 7)	(n = 7)	(n = 6)	(n = 6)
Week 1	1.9 ± 1.6	1.6 ± 1.0	1.8 ± 2.2	2.6 ± 1.6
Week 4	1.0 ± 0.6	1.3 ± 0.5	1.7 ± 1.4	1.7 ± 1.1
Intraobserver	(n = 7)	(n = 7)	(n = 6)	(n = 6)
Week 1	0.9 ± 0.8	0.6 ± 0.3	0.8 ± 0.7	0.9 ± 0.7
Week 4	0.5 ± 0.5	0.8 ± 0.8	0.8 ± 0.5	1.4 ± 0.9
Intrasubject	(n = 2)	(n = 2)	(n = 3)	(n = 3)
Week 4	0.8 ± 0.8	1.5 ± 0.4	3.6 ± 0.2	5.5 ± 0.8

Values are means ± SD. n indicates number of animals.

TABLE 4. Comparison of CT-Based Measurements and Hemodynamic Measurements at 4 Weeks Postsurgery

	CT Measurements		Hemodynamic Measurements	
Functional Measurements	**Sham (n = 7)**	**MI (n = 6)**	**Sham (n = 7)**	**MI (n = 6)**
LVDV (μL)	61 ± 10	178 ± 35	26 ± 8	29 ± 10
LVSV (μL)	23 ± 7	139 ± 45	12 ± 6	21 ± 7
SV (μL)	39 ± 6	38 ± 15	14 ± 7	7 ± 5
EF (%)	63 ± 7	23 ± 12	54 ± 20	26 ± 15
CO (mL/min)	20 ± 2	19 ± 7	5 ± 3	2 ± 1
dP/dt_{max} (mm Hg · s)	—	—	7321 ± 948	3456 ± 1032
dP/dt_{min} (mm Hg · s)	—	—	5969 ± 1070	3102 ± 861
Heart rate (bpm)	511 ± 30	505 ± 32	360 ± 80	281 ± 48

Values are means ± SD. n indicates number of animals.
dP/dt_{max} indicates maximum derivative of change in systolic pressure over time; dP/dt_{min}, maximum derivative of change in diastolic pressure over time.

derived LV volume measurements, because of the accepted underestimation and large variability of volume measurements made invasively by pressure-conductance catheters.[2,3] The use of different anesthetics when comparing micro-CT to catheterization was not ideal; however, our aim in using inhalation anesthetics during CT scanning was to emphasize the low invasiveness of the CT approach. Using an injectable anesthetic would have made controlling the depth of anesthesia difficult, as well as increasing the invasiveness of the procedure. In addition, the hemodynamic measurements were made on the same day as the scanning occurred, but after the administration of a second (injectable) anesthetic agent, which resulted in further lowering the heart rates during the procedure. The number of animals in the study was small, but important functional parameters could be followed over time with sufficient statistical power, indicating the effectiveness of the technique to follow cardiac remodeling.

Summary and Implications

The present work demonstrates that retrospectively gated micro-CT precisely defines the differences in heart function and volume between sham and MI animals. This methodology has the ability of following individual animals over the entire study, enabling the tracking of small changes in cardiac remodeling that may not be evident when averaging a group of mice. Reproducibility studies show low variability during analysis (inter- and intraobserver). The rapid acquisition of dynamic 3D images also makes the technique highly suitable for large throughput phenotyping studies. Furthermore, the retrospectively gated micro-CT technique can be combined with the injection of a conventional contrast agent, as suggested by Nahrendorf et al[23] to identify areas of infarction, where the contrast agent extravasates over time. Ultimately, retrospectively gated micro-CT has the potential to become an important tool for following disease progression and disease regression, after the administration of various experimental therapeutic agents.

ACKNOWLEDGMENTS

The authors thank Andrew Wheatley for performing CT image reconstructions, Lisa MacKenzie for handling the animals during scanning, and Joy Dunmore-Buyze and Steven Armitage for their help with image analysis.

REFERENCES

1. Lips DJ, van der Nagel T, Steendijk P, et al. Left ventricular pressure-volume measurements in mice: comparison of closed-chest versus open-chest approach. *Basic Res Cardiol*. 2004;99:351–359.
2. Jacoby C, Molojavyi A, Flogel U, et al. Direct comparison of magnetic resonance imaging and conductance microcatheter in the evaluation of left ventricular function in mice. *Basic Res Cardiol*. 2006;101:87–95.
3. Nielsen JM, Kristiansen SB, Ringgaard S, et al. Left ventricular volume measurement in mice by conductance catheter: evaluation and optimization of calibration. *Am J Physiol Heart Circ Physiol*. 2007;293:H534–H540.
4. Schneider JE, Cassidy PJ, Lygate C, et al. Fast, high-resolution in vivo cine magnetic resonance imaging in normal and failing mouse hearts on a vertical 11.7 T system. *J Magn Reson Imaging*. 2003;18:691–701.
5. Schneider JE, Wiesmann F, Lygate CA, et al. How to perform an accurate assessment of cardiac function in mice using high-resolution magnetic resonance imaging. *J Cardiovasc Magn Reson*. 2006;8:693–701.
6. Gilson WD, Yang Z, French BA, et al. Measurement of myocardial mechanics in mice before and after infarction using multislice displacement-encoded MRI with 3D motion encoding. *Am J Physiol Heart Circ Physiol*. 2005;288:H1491–1497.
7. Liu W, Ashford MW, Chen J, et al. MR tagging demonstrates quantitative differences in regional ventricular wall motion in mice, rats, and men. *Am J Physiol Heart Circ Physiol*. 2006;291:H2515–2521.
8. Zhou R, Pickup S, Glickson JD, et al. Assessment of global and regional myocardial function in the mouse using cine and tagged MRI. *Magn Reson Med*. 2003;49:760–764.
9. Bishop J, Feintuch A, Bock NA, et al. Retrospective gating for mouse cardiac MRI. *Magn Reson Med*. 2006;55:472–477.
10. Hiba B, Richard N, Janier M, et al. Cardiac and respiratory double self-gated cine MRI in the mouse at 7 T. *Magn Reson Med.* 2006;55:506–513.
11. Zhou YQ, Foster FS, Nieman BJ, et al. Comprehensive transthoracic cardiac imaging in mice using ultrasound biomicroscopy with anatomical confirmation by magnetic resonance imaging. *Physiol Genomics*. 2004;18:232–244.
12. Costandi PN, Frank LR, McCulloch AD, et al. Role of diastolic properties in the transition to failure in a mouse model of the cardiac dilatation. *Am J Physiol Heart Circ Physiol*. 2006;291:H2971–2979.
13. Saraste A, Kyto V, Saraste M, et al. Coronary flow reserve and heart failure in experimental coxsackievirus myocarditis. A transthoracic Doppler echocardiography study. *Am J Physiol Heart Circ Physiol*. 2006;291:H871–875.
14. Neilan TG, Jassal DS, Perez-Sanz TM, et al. Tissue Doppler imaging predicts left ventricular dysfunction and mortality in a murine model of cardiac injury. *Eur Heart J*. 2006;27:1868–1875.

15. Sebag IA, Handschumacher MD, Ichinose F, et al. Quantitative assessment of regional myocardial function in mice by tissue Doppler imaging: comparison with hemodynamics and sonomicrometry. *Circulation*. 2005;111:2611–2616.
16. Cherin E, Williams R, Needles A, et al. Ultrahigh frame rate retrospective ultrasound microimaging and blood flow visualization in mice in vivo. *Ultrasound Med Biol*. 2006;32:683–691.
17. Feintuch A, Zhu Y, Bishop J, et al. 4D cardiac MRI in the mouse. *NMR Biomed*. 2007;20:360–365.
18. Dawson D, Lygate CA, Saunders J, et al. Quantitative 3-dimensional echocardiography for accurate and rapid cardiac phenotype characterization in mice. *Circulation*. 2004;110:1632–1637.
19. Xu M, Uemura R, Dai Y, et al. In vitro and in vivo effects of bone marrow stem cells on cardiac structure and function. *J Mol Cell Cardiol.* 2007;42:441–448.
20. Semsarian C, Ahmad I, Giewat M, et al. The L-type calcium channel inhibitor diltiazem prevents cardiomyopathy in a mouse model. *J Clin Invest*. 2002;109:1013–1020.
21. Alvarez BV, Kieller DM, Quon AL, et al. Cardiac hypertrophy in anion exchanger 1-null mutant mice with severe hemolytic anemia. *Am J Physiol Heart Circ Physiol*. 2007;292:H1301–1312.
22. Badea CT, Fubara B, Hedlund LW, et al. 4-D micro-CT of the mouse heart. *Mol Imaging*. 2005;4:110–116.
23. Nahrendorf M, Badea C, Hedlund LW, et al. High-resolution imaging of murine myocardial infarction with delayed-enhancement cine micro-CT. *Am J Physiol Heart Circ Physiol*. 2007;292:H3172–3178.
24. Schneider JE, Hulbert KJ, Lygate CA, et al. Long-term stability of cardiac function in normal and chronically failing mouse hearts in a vertical-bore MR system. *Magma*. 2004;17:162–169.
25. Drangova M, Ford NL, Detombe SA, et al. Fast retrospectively gated quantitative four-dimensional (4D) cardiac micro computed tomography imaging of free-breathing mice. *Invest Radiol*. 2007;42:85–94.
26. Bartling SH, Stiller W, Grasruck M, et al. Retrospective motion gating in small animal CT of mice and rats. *Invest Radiol*. 2007;42:704–714.
27. Feng Q, Lu X, Jones DL, et al. Increased inducible nitric oxide synthase expression contributes to myocardial dysfunction and higher mortality after myocardial infarction in mice. *Circulation*. 2001;104:700–704.
28. Ford NL, Graham KC, Groom AC, et al. Time-course characterization of the computed tomography contrast enhancement of an iodinated blood-pool contrast agent in mice using a volumetric flat-panel equipped computed tomography scanner. *Invest Radiol*. 2006;41:384–390.
29. Ford NL, Nikolov HN, Norley CJ, et al. Prospective respiratory-gated micro-CT of free breathing rodents. *Med Phys*. 2005;32:2888–2898.
30. Du LY, Umoh J, Nikolov HN, et al. A quality assurance phantom for the performance evaluation of volumetric micro-CT systems. *Phys Med Biol*. 2007;52:7087–7108.
31. Otsu N. A threshold selection method from gray-level histograms. *IEEE Trans Syst Man Cybern (USA)*. 1979;SMC-9:62–66.
32. Wiesmann F, Ruff J, Engelhardt S, et al. Dobutamine-stress magnetic resonance microimaging in mice: acute changes of cardiac geometry and function in normal and failing murine hearts. *Circ Res*. 2001;88:563–569.
33. Janssen B, Debets J, Leenders P, et al. Chronic measurement of cardiac output in conscious mice. *Am J Physiol Regul Integr Comp Physiol*. 2002;282:R928–935.
34. Mayo JR, Aldrich J, Muller NL. Radiation exposure at chest CT: a statement of the Fleischner Society. *Radiology*. 2003;228:15–21.
35. Campbell J, Kalra MK, Rizzo S, et al. Scanning beyond anatomic limits of the thorax in chest CT: findings, radiation dose, and automatic tube current modulation. *AJR Am J Roentgenol*. 2005;185:1525–1530.
36. van Rongen E, Travis EL, Thames HD Jr. Repair rate in mouse lung after clinically relevant radiation doses per fraction. *Radiat Res*. 1995; 141:74–78.
37. Vegesna V, Withers HR, Taylor JM. Repair kinetics of mouse lung. *Radiother Oncol*. 1989;15:115–123.
38. Takuma S, Suehiro K, Cardinale C, et al. Anesthetic inhibition in ischemic and nonischemic murine heart: comparison with conscious echocardiographic approach. *Am J Physiol Heart Circ Physiol*. 2001; 280:H2364–2370.
39. Tan TP, Gao XM, Krawczyszyn M, et al. Assessment of cardiac function by echocardiography in conscious and anesthetized mice: importance of the autonomic nervous system and disease state. *J Cardiovasc Pharmacol*. 2003;42:182–190.
40. Ishizaka S, Sievers RE, Zhu BQ, et al. New technique for measurement of left ventricular pressure in conscious mice. *Am J Physiol Heart Circ Physiol*. 2004;286:H1208–1215.
41. Roth DM, Swaney JS, Dalton ND, et al. Impact of anesthesia on cardiac function during echocardiography in mice. *Am J Physiol Heart Circ Physiol*. 2002;282:H2134–2140.
42. Bairey CN, de Yang L, Berman DS, et al. Comparison of physiologic ejection fraction responses to activities of daily living: implications for clinical testing. *J Am Coll Cardiol*. 1990;16:847–854.
43. Becker LC, Pepine CJ, Bonsall R, et al. Left ventricular, peripheral vascular, and neurohumoral responses to mental stress in normal middle-aged men and women. Reference Group for the Psychophysiological Investigations of Myocardial Ischemia (PIMI) Study. *Circulation*. 1996; 94:2768–2777.
44. Yang F, Liu YH, Yang XP, et al. Myocardial infarction and cardiac remodelling in mice. *Exp Physiol*. 2002;87:547–555.